MEDICAL SCIENCE MONITOR

ANIMAL STUDY

e-ISSN 1643-3750
© Med Sci Monit, 2016; 22: 2751-2760
DOI: 10.12659/MSM.898105

Received: 2016.02.18
Accepted: 2016.03.31
Published: 2016.08.04

Renal Sympathetic Denervation in Rats Ameliorates Cardiac Dysfunction and Fibrosis Post-Myocardial Infarction Involving MicroRNAs

Authors' Contribution:
Study Design A
Data Collection B
Statistical Analysis C
Data Interpretation D
Manuscript Preparation E
Literature Search F
Funds Collection G

ABCE 1,2,3 Xiaoxin Zheng
BCF 1,2,3 Xiaoyan Li
BC 1,2,3 Yongnan Lyu
CDF 1,2,3 Yiyu He
BD 1,2,3 Weiguo Wan
ABFG 1,2,3 Xuejun Jiang

1 Department of Cardiology, Renmin Hospital of Wuhan University, Wuhan, Hubei, P.R. China
2 Cardiovascular Research Institute, Wuhan University, Wuhan, Hubei, P.R. China
3 Hubei Key Laboratory of Cardiology, Wuhan, Hubei, P.R. China

Corresponding Author: Xuejun Jiang, e-mail: xjjiang@whu.edu.cn
Source of support: This work was supported by research grants (2042015kf0074) from the Fundamental Research Funds for the Central Universities of China

Background: The role of renal sympathetic denervation (RSD) in ameliorating post-myocardial infarction (MI) left ventricular (LV) fibrosis via microRNA-dependent regulation of connective tissue growth factor (CTGF) remains unknown.

Material/Methods: MI and RSD were induced in Sprague–Dawley rats by ligating the left coronary artery and denervating the bilateral renal nerves, respectively. Norepinephrine, renin, angiotensin II and aldosterone in plasma, collagen, microRNA21, microRNA 101a, microRNA 133a and CTGF in heart tissue, as well as cardiac function were evaluated six weeks post-MI.

Results: In the RSD group, parameters of cardiac function were significantly improved as evidenced by increased LV ejection fraction ($p<0.01$), LV end-systolic diameter ($p<0.01$), end-diastolic diameter ($p<0.05$), LV systolic pressure ($p<0.05$), maximal rate of pressure rise and decline (dP/dt_{max} and dP/dt_{min}, $p<0.05$), and decreased LV end-diastolic pressure ($p<0.05$) when compared with MI rats. Further, reduced collagen deposition in peri-infarct myocardium was observed in RSD-treated rats along with higher microRNA101a and microRNA133a ($p<0.05$) and lower microRNA21 expression ($p<0.01$) than in MI rats. CTGF mRNA and protein levels were decreased in LV following RSD ($p<0.01$), accompanied by decreased expression of norepinephrine, renin, angiotensin II and aldosterone in plasma ($p<0.05$) compared with untreated MI rats.

Conclusions: The potential therapeutic effects of RSD on post-MI LV fibrosis may be partly mediated by inhibition of CTGF expression via upregulation of microRNA 101a and microRNA 133a and downregulation of microRNA21.

MeSH Keywords: Connective Tissue Growth Factor • MicroRNAs • Myocardial Infarction

Full-text PDF: http://www.medscimonit.com/abstract/index/idArt/898105

Indexed in: [Current Contents/Clinical Medicine] [SCI Expanded] [ISI Alerting System] [ISI Journals Master List] [Index Medicus/MEDLINE] [EMBASE/Excerpta Medica] [Chemical Abstracts/CAS] [Index Copernicus]

Background

Heart failure (HF) due to myocardial infarction (MI) is associated with a high mortality rate. Cardiac fibrosis plays a key role in the progressive deterioration of ventricular function in the development of heart failure after MI [1]. It is characterized by excessive deposition of extracellular matrix (ECM) proteins, such as Collagen I, Collagen III, fibronectin, elastin, and fibrin. Collagen synthesis contributes to collagen accumulation, leading to cardiac fibrosis and myocardial stiffness. Among the mechanisms that lead to cardiac fibrosis and remodeling, hyper-stimulation of the sympathetic nervous system (SNS) and renin-angiotensin-aldosterone system (RAAS) are two primary mechanisms [2] in the setting of hypertension-induced heart failure.

Renal sympathetic denervation (RSD), which was introduced as a technique that protects against heart failure via denervation of afferent and efferent renal sympathetic nerve fibers, plays a pivotal role in the regulation of neurohumoral mechanisms, including SNS and RAAS [3–5]. Animal studies have shown that RSD inhibits ventricular remodeling in animals with heart failure [6,7] and attenuates the progression of left ventricular hypertrophy in rats caused by spontaneous hypertension [8]. These studies suggest that the positive role of RSD on neurohumoral activities may be further validated as an effective treatment option in heart failure after MI. The underlying mechanisms need further investigation.

Mature microRNAs are endogenous, non-coding small RNAs, 22nt in length, which silence genes by inhibiting mRNA translation or promoting mRNA degradation. They play key roles in fibrosis, proliferation, and cell death of cardiac tissue [9], especially in regulating cardiac fibrosis. For example, microRNA-21 promotes the progression of fibrosis [10], while microRNA-101a and microRNA-133a have been identified as regulators of connective tissue growth factor (CTGF) by decreasing collagen synthesis [11]. CTGF is a secreted protein which is a powerful inducer of ECM synthesis and fibrotic disorders [12,13]. The ECM and fibrosis of the heart are known to play a pivotal role in myocardial remodeling caused by excessive activation of SNS and RAAS [14]. During cardiac remodeling, both cardiac myocytes and fibroblasts secrete CTGF via regulation of growth factors and microRNAs [11]. It is important to elucidate the underlying mechanisms and develop new therapeutic strategies for MI-induced LV remodeling. We hypothesized that RSD might act against the progression of cardiac fibrosis after MI by regulating microRNAs and growth factors of the myocardium. Therefore, we investigated the therapeutic effects of RSD on cardiac fibrosis and discussed the potential mechanisms underlying the functional and morphological alterations in the peri-infarct area of myocardial tissue using a rat MI model.

Material and Methods

Ethics statement

This study was carried out in strict accordance with the "Guide for the Care and Use of Laboratory Animals" published by the US National Institutes of Health (NIH Publication No. 85-23, revised 1996). All animal experimental protocols were approved by the Institutional Animal Care Committee at Wuhan University.

Animals

Seventy-one male Sprague-Dawley (SD) rats (180–200 g) were purchased from the Beijing HFK Bioscience CO., LTD (Beijing, China). Animals were maintained under standard animal room conditions at a room temperature of 21±2°C and humidity of 60–65% in a 12:12 light/dark cycle. A standard rat diet containing 0.3% NaCl and tap water was given *ad libitum* throughout the experimental period. All efforts were made to minimize animal suffering.

Group setting

Seventy-one SPF male SD rats were randomly divided into four groups: normal animals serving as a control group (n=15), animals treated with renal sympathetic denervation (RSD group, n=18), MI group (n=18), and animals treated with RSD seven days post-MI (MI7d+RSD group, n=20).

Myocardial infarction model

MI was induced by ligation of the left coronary artery under combined intraperitoneal anesthesia (40 mg/kg pentobarbital sodium). Rats were intubated and ventilated by a volume-regulated respirator during surgery. The left coronary artery was ligated 2 to 3 mm from its origin using a 6-0 prolene suture via left thoracotomy between the fourth and the fifth intercostal space. Subsequently, the infarcted area of LV was paled immediately. The thorax was closed and the animals were allowed to recover. Intramuscular injection of penicillin 400,000 U was administered daily for three days to prevent infection.

Renal sympathetic denervation

RSD was performed under intraperitoneal anesthesia (40 mg/kg pentobarbital sodium). Both kidneys were surgically denervated by cutting all visible nerves from the renal arteries and veins under an operating microscope. The vessels were then coated with a 20% phenol/ethanol solution for 10–15 minutes. The renal sympathetic nerves were electrically stimulated for 20–30 seconds to evaluate the effects of RSD (Grass S48 nerve stimulator, 0.2 ms, 15 V, 10 Hz). In normal rats, the blood pressure increased by 5–10 mmHg, heart rate increased by 8–15

Indexed in: [Current Contents/Clinical Medicine] [SCI Expanded] [ISI Alerting System] [ISI Journals Master List] [Index Medicus/MEDLINE] [EMBASE/Excerpta Medica] [Chemical Abstracts/CAS] [Index Copernicus]

bpm, and the kidney became paler after electrical stimulation. Changes in blood pressure, heart rate, or kidney color were absent in animals after RSD.

Echocardiography

All the experimental animals were anaesthetized under 40 mg/kg pentobarbital anesthesia for echocardiography before and at six weeks after MI surgery. The echocardiographic measurements were performed using a 15 MHz ultraband sector probe (SONOS 5500, Hewlett-Packard, Andover, MA). LV ejection fraction (EF), heart rate, LV end-systolic diameter (ESD) and LV end-diastolic diameter (EDD) were measured in the short-axis M-mode left parasternal projection at the mid-portion of the left ventricle. All the procedures and analyses were performed by an experienced researcher in a blinded fashion.

Hemodynamics

After echocardiographic data collection, a Millar Microtip catheter (SPR-407, Millar Institute, Houston, TX, USA) was introduced from the right carotid artery into the left ventricle. With the rat anesthetized lightly and breathing spontaneously, LV systolic pressure (LVSP), LV end-diastolic pressure (LVEDP), maximum and minimum alterations in LV pressure (dP/dtmax and dP/dt min, respectively) were measured.

Neurohormonal assays

After echocardiography at six weeks post-MI or RSD, blood samples were drawn from the inferior vena cava into tubes containing EDTA, immediately centrifuged at 3000 rpm for 10 minutes at 4°C (Avanti J-E; Beckman Coulter, Brea, CA, USA), separated into microtubes and stored at –80°C until used for analysis. Plasma norepinephrine (NE), renin, angiotensin II (Ang II), and aldosterone (ALD) levels were measured using ELISA kits (Rat kit, Abnova GmbH Inc., Heidelberg, Germany).

Masson's trichrome staining and infarct size of left ventricles

Six weeks post-MI or RSD, the rats were sacrificed using an excess intraperitoneal anesthesia (60–70 mg/kg pentobarbital sodium). Masson's trichrome staining was used to evaluate collagen deposition. The myocardial interstitial collagen volume fractions were determined using image analysis software (Rockville, MD, USA). Results were presented as the ratio of collagen surface area stained blue to the myocardial surface area. Infarct size was assessed by examining images obtained at low magnification and calculated as the ratio of the length of the infarcted endocardial circumference to the entire endocardial circumference, as previously reported [15].

Immunohistochemistry of Collagen I, Collagen III, and CTGF expression in left ventricle

The left ventricles were isolated as needed, embedded in paraffin, and sectioned at a thickness of 5 μM. The paraffin-embedded sections were incubated overnight at 4°C with primary antibodies (CTGF, Abcam Ltd., 1:400; Collagen I, Abcam Ltd., 1:300; Collagen III, Abcam Ltd., 1:100) and visualized with horseradish peroxidase-conjugated IgG (1:100; Sigma-Aldrich) for one hour, respectively, at room temperature before computerized image analysis (AIS Imaging, Ontario, Canada). Negative control sections were incubated in the absence of primary antibody.

Real-time reverse-transcription polymerase chain reaction (RT-PCR) analysis

The total RNA was isolated from peri-infarct area of myocardial tissue with TRIzol (Invitrogen, Carlsbad, CA). To determine the levels of CTGF, Collagen I, Collagen III, and β-actin, real-time RT-PCR was performed using 1 mg total RNA as described previously [16]. The primer sequences were as follows:
miR-101a, 3p loop primer: 5'-GTCGTATCCAGTGCAGGG TCCGAG GTATTCGCACTGGATACGAC TTCAGTTA,
miR-101a, 3p F primer: TGCGCTACAGTACTGTGATAA;
miR-133a, 3p loop primer: 5'-GTCGTATCCAGTGCAGGGTCC GAGGTATTCGCACTGGATACGAC CAGCTGGT,
miR-133a, 3p F primer: TGCGCTTTGGTCCCCTTCAACC;
miR-21, 5p loop primer: 5'-GTCGTATCCAGTGCAGGGTCC GAGGTATTCGCACTGGATACGAC TCAACATC,
miR-21, 5p F primer: TGCGCTAGCTTATCAGACTGAT;
Collagen I, forward, 5'-CGAGTATGGAAGCGAAGGT-3',
Collagen I, reverse, 5'- CCACAAGCGTGCTGTAGGT-3';
collage III, forward, 5'- ATTGCTGGAGTTGGAGGTGA-3',
collage III, reverse, 5'-TGAGTTCAGGGTGGCAGAAT-3'
CTGF, forward, 5'-GTCTTCGGTGGGTCCGTGTA-3',
CTGF, reverse, 5'-CCACAAGCGTGCTGTAGGT -3' and
β-actin, forward, 5'- CACGATGGAGGGGCCGGACTCATC-3',
and β-actin, reverse, 5'- TAAAGACCTCTATGCCAACACAGT-3'.

The PCR products were subjected to gel electrophoresis using 1.5% agar containing 0.5 mg/mL ethidium bromide. All data were quantified using the comparative cycle threshold method, normalized to β-actin.

Western blot analysis

Protein extraction and protein assay were performed from the left ventricle using the procedure described previously [16] followed by fractionation of 50 mg proteins on a 10% SDS-polyacrylamide gel and electrophoretic transfer to pure nitrocellulose blotting membranes. The blots were incubated with primary antibody overnight using GAPDH as the control. The antibodies and dilutions were as follows: CTGF (Santa Cruz

Indexed in: [Current Contents/Clinical Medicine] [SCI Expanded] [ISI Alerting System] [ISI Journals Master List] [Index Medicus/MEDLINE] [EMBASE/Excerpta Medica] [Chemical Abstracts/CAS] [Index Copernicus]

Table 1. Body weight, heart rate and infarct size obtained six weeks post-MI.

	Control (n=18)	RSD (n=18)	MI (n=18)	MI7d+RSD (n=20)
Body weight (g)	391±10.2	384±8.4	368±9.2	352±9.3
Heart rate (bpm)	434.5±19.8	436.2±15.7	446.5±14.8	433.2±16.6
Infarct size (%)			39.2±2.5	37.2±1.9

Values are means ± standard deviation. Control – normal group; RSD – renal sympathetic denervation; MI – myocardial infarction; MI7d+RSD – rats treated with RSD performed seven days post-MI. Infarct size was identified by dividing the total necrotic area of the left ventricle by the total left ventricular slice area. * P<0.05 *vs.* Control, # P<0.05 *vs.* MI.

Table 2. Renin, angiotensin II, aldosterone and norepinephrine levels treated with RSD.

	Control	RSD	MI	MI7d+RSD
Renin (ng/L)	232.1±10.3	219.5±8.9	1321.7±89.1*	332.4±18.4#
Angiotensin II (ng/L)	132.3±6.9	146.3±7.2	1245.2±68.3*	214.3±9.9#
Aldosterone (ng/L)	190.6±8.2	169.3±7.7	1078.2±73.5*	245.5±12.2#
Norepinephrine (ng/L)	514.8±30.3	599.1±29.8	1453.2±83.3*	692.3±38.4#

Control – normal group; RSD – renal sympathetic denervation; MI – myocardial infarction; MI7d+RSD – rats treated with RSD performed seven days post-MI. Data were shown as mean ± standard deviation. * P<0.05 *vs.* either control or RSD group; # P<0.05 *vs.* MI group.

Biotechnology, 1:400), Collagen I (Abcam Ltd., 1:1000), Collagen III (Santa Cruz Biotechnology, 1:6000), and GAPDH (anti-GAPDH Mouse Monoclonal Antibody; Abbkine Inc. USA, 1:1000). The corresponding secondary antibody (goat anti-rabbit immunoglobulin G, Santa Cruz Biotechnology) was incubated at 37°C for two hours. The blots were visualized and quantified by measuring the band intensity.

Statistical analysis

Data are presented as means ±SD, and the differences were tested for significance using analysis of variance (ANOVA), followed by the Bonferroni test when appropriate. Results were considered statistically significant when $p<0.05$.

Results

Body weight, heart rate, and left ventricular infarct size after MI

Anesthesia-related accidents contributed to 2.8% (2/71) of deaths and heart failure to 16.9% (12/71) of deaths post-MI. Blood loss post-RSD resulted in 7.0% (5/71) of deaths. Seven days post-MI, RSD was performed on the surviving 14 rats, with 100% survival. No significant difference in the ratio of weight and infarct area was seen in each group six weeks post-MI (Table 1).

Effects of RSD on the plasma renin, angiotensin II, aldosterone and norepinephrine levels

Compared with the baseline values of the control group, RSD did not alter the plasma renin, angiotensin II, aldosterone, or norepinephrine levels after six weeks. Compared with the values in the MI group, a decrease in plasma renin, angiotensin II, and aldosterone levels by 74.8%, 82.8%, and 77.2% was observed in the RSD treatment group, respectively (Table 2, $p<0.05$). MI-induced increase in plasma levels of noradrenaline was reduced by 52.3% after RSD treatment (Table 2, $p<0.05$).

RSD improves cardiac function six weeks post-MI

Six weeks post-MI, LVESD and LVEDD of the MI group were significantly increased (Figure 1, $p<0.01$, $p<0.05$, respectively). LVEF was significantly reduced (Figure 1, $p<0.01$) compared with the control group. RSD decreased LVESD and LVEDD (Figure 1, $p<0.01$, $p<0.05$, respectively), while LVEF was increased compared with the MI group (Figure 1, $p<0.01$).

Hemodynamic parameters of the four groups at six weeks post-surgery are shown in Figure 2. LVEDP was higher (Figure 2A, $p<0.05$) and LVSP, dP/dtmax, and dP/dtmin were lower in untreated MI rats compared with the control group (Figure 2B–2D, $p<0.05$). LVEDP was decreased (Figure 2A, $p<0.05$), while LVSP, dP/dtmax, and dP/dtmin were increased in rats treated with RSD compared with MI rats (Figure 2B–2D, $p<0.05$).

Indexed in: [Current Contents/Clinical Medicine] [SCI Expanded] [ISI Alerting System] [ISI Journals Master List] [Index Medicus/MEDLINE] [EMBASE/Excerpta Medica] [Chemical Abstracts/CAS] [Index Copernicus]

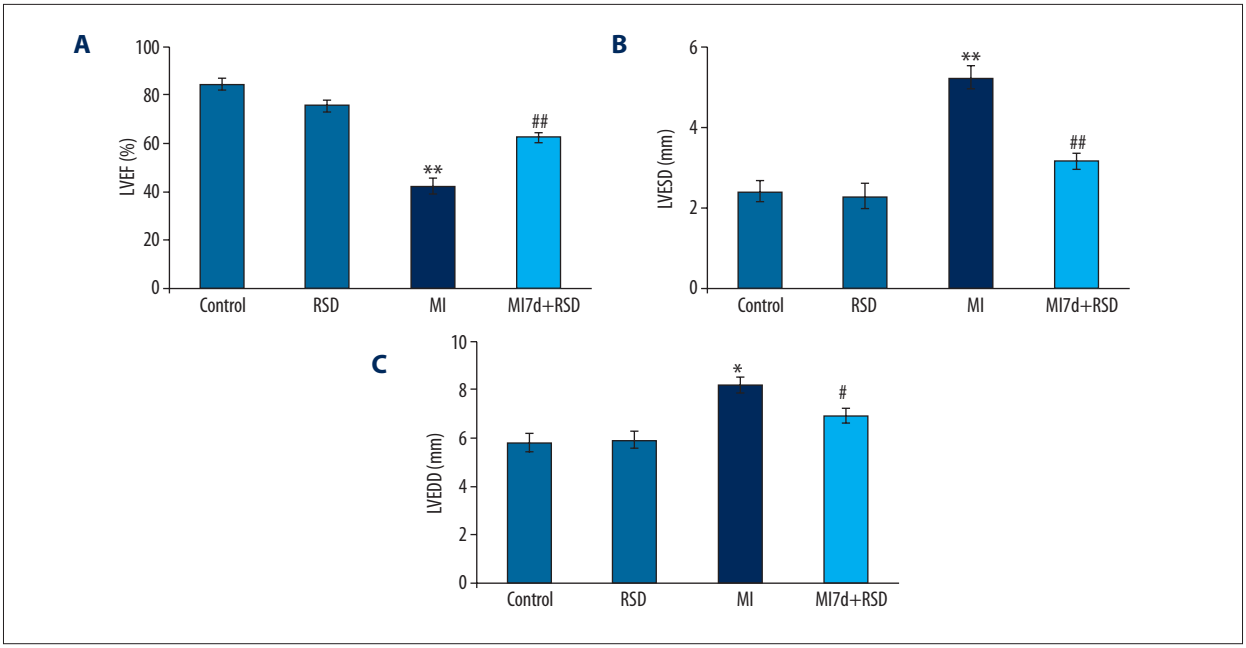

Figure 1. (**A–C**) Echocardiographic parameters at six weeks post-MI. Control – normal group; RSD – renal sympathetic denervation; MI – myocardial infarction; MI7d+RSD – rats treated with RSD performed seven days post-MI. LVEF – left ventricular ejection fraction; LVESD and LVEDD – left ventricular end-systolic diameter and left ventricular end-diastolic diameter, respectively. Data are expressed as mean ±SD. * $p<0.05$, ** $p<0.01$ *vs.* either Control or RSD group, respectively; # $p<0.05$, ## $p<0.01$ *vs.* MI group, respectively.

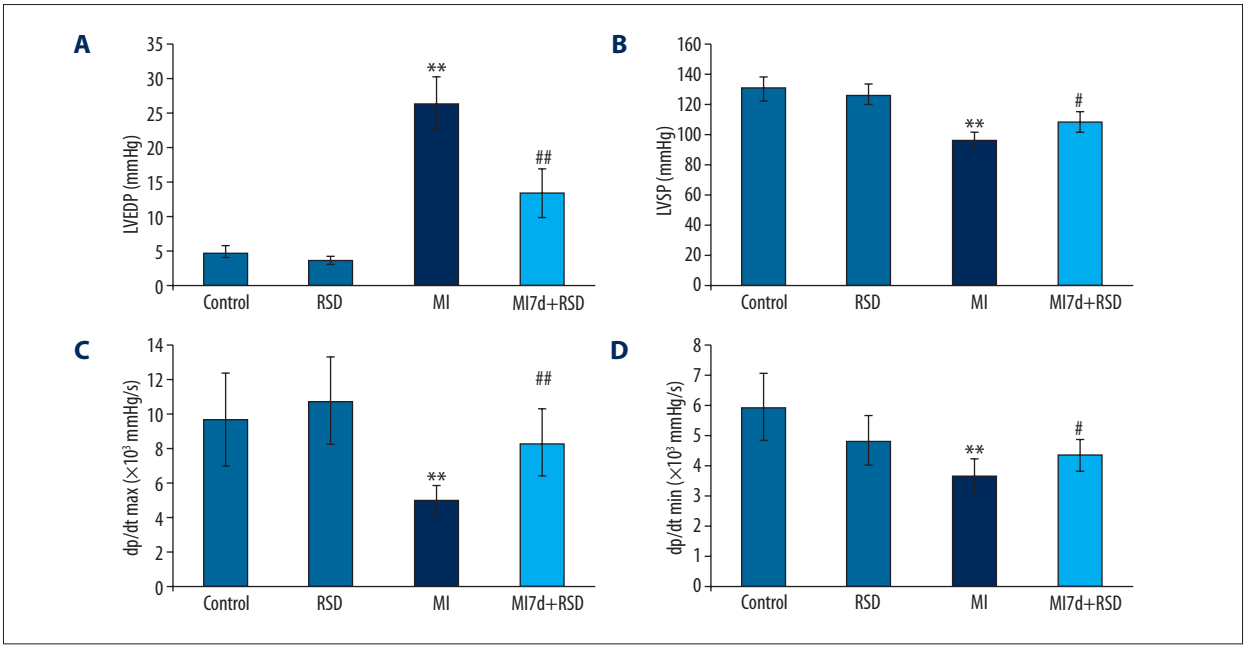

Figure 2. (**A–D**) Hemodynamic measurements at six weeks post-MI. Control, normal group; RSD, renal sympathetic denervation; MI – myocardial infarction; MI7d+RSD, rats treated with RSD performed seven days post-MI. LVEDP – left ventricular end-diastolic pressure; LVSP – left ventricular systolic pressure; dP/dtmax – maximal rate of pressure rise; dP/dt min – maximal rate of pressure decline. Data are expressed as mean ±SD. ** $p<0.01$ *vs.* either Control or RSD group; # $p<0.05$, ## $p<0.01$ *vs.* MI group.

Indexed in: [Current Contents/Clinical Medicine] [SCI Expanded] [ISI Alerting System] [ISI Journals Master List] [Index Medicus/MEDLINE] [EMBASE/Excerpta Medica] [Chemical Abstracts/CAS] [Index Copernicus]

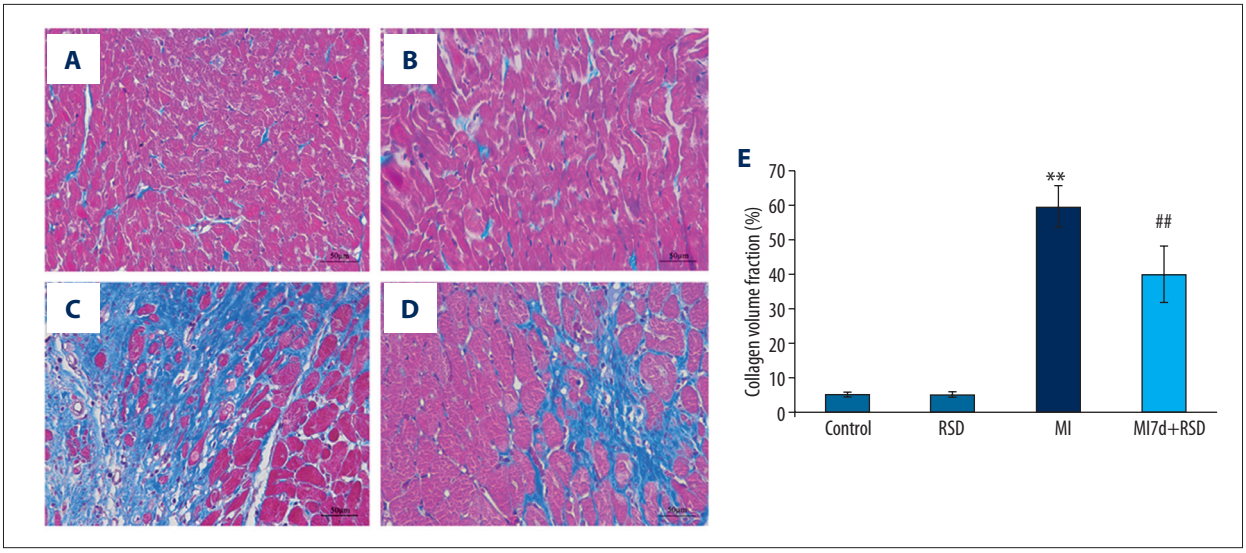

Figure 3. Histological specimens from the border zone of the infarcted left ventricle region were stained with Masson's richrome in each group. (**A–D**) Show representative micrographs (magnification: 400×) and (**E**) shows that the left ventricular sections in the RSD group show less fibrosis than in the MI group. Data are presented as mean ±standard deviation; ** $p<0.01$ *vs.* either Control or RSD group, ## $p<0.001$ *vs.* MI group.

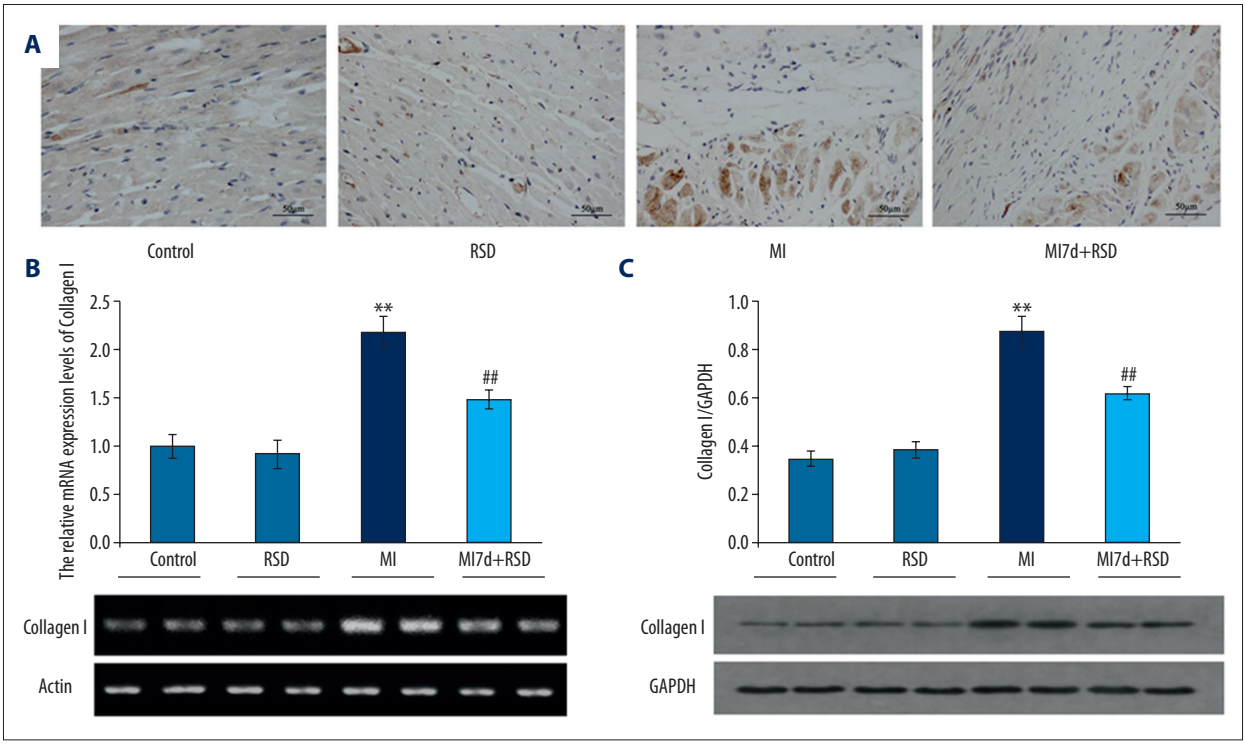

Figure 4. Changes in mRNA and protein levels of Collagen I in left ventricle (LV) six weeks post-MI. (**A**) Immunostaining of Collagen I, brown stain, 400×. (**B**) Relative expression of Collagen I mRNA in LV. (**C**) Western blot of Collagen I. Densitometric data are presented as mean ± standard deviation. Compared with normal rats, the protein and mRNA expression of Collagen I is upregulated in the peri-infarct area of LV of MI rats at six weeks, which is significantly reduced after renal sympathetic denervation. Data are presented as mean ±SD. ** $p<0.01$ *vs.* either control or RSD group; ## $p<0.01$ *vs.* MI group.

Indexed in: [Current Contents/Clinical Medicine] [SCI Expanded] [ISI Alerting System] [ISI Journals Master List] [Index Medicus/MEDLINE] [EMBASE/Excerpta Medica] [Chemical Abstracts/CAS] [Index Copernicus]

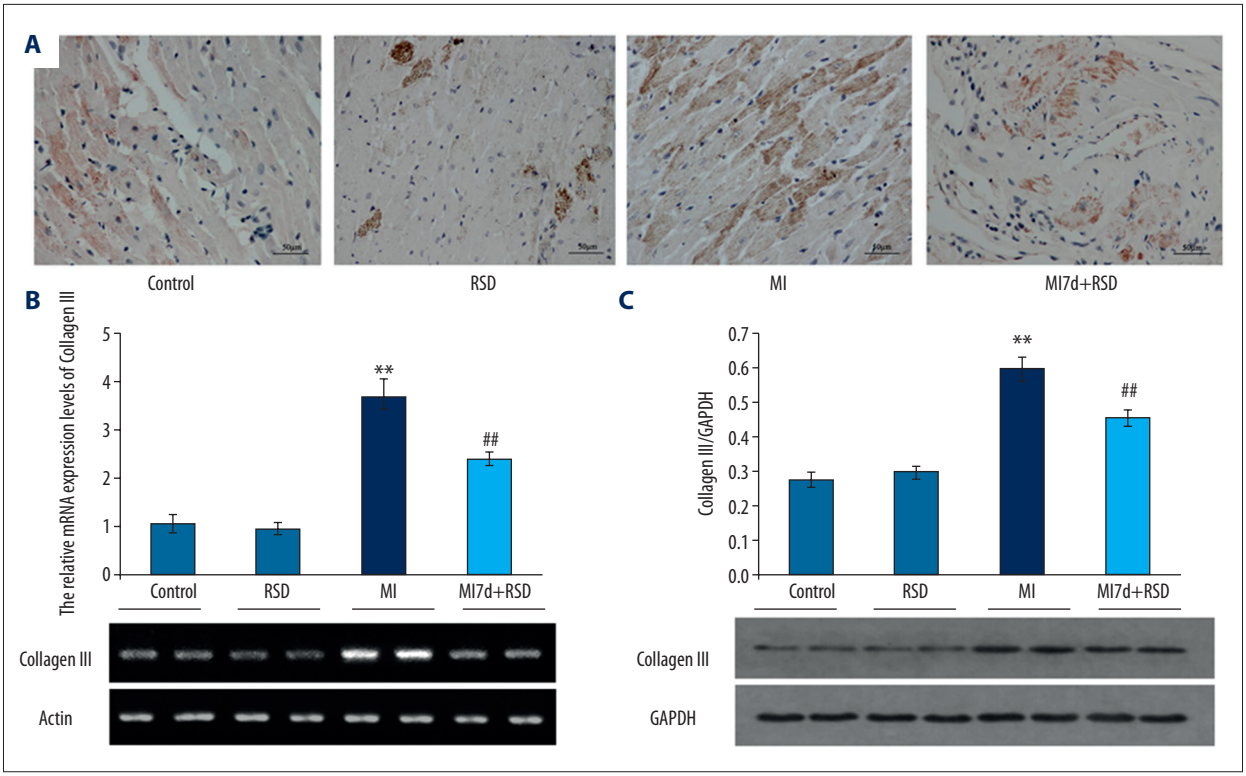

Figure 5. Changes in mRNA and protein levels of Collagen III in left ventricle (LV) six weeks post-MI. (**A**) Immunostaining of Collagen III, brown stain, 400×; (**B**) Relative expression of Collagen I mRNA in LV; (**C**) Western blot of Collagen III. Compared with the normal rats, the protein and mRNA expression of Collagen III is upregulated in the peri-infarct area of LV of MI rats at six weeks, which is significantly reduced after renal sympathetic denervation. Data are presented as mean ± standard deviation. ** $p<0.01$ *vs.* either control or RSD group; ## $p<0.01$ *vs.* MI group.

RSD decreases collagen deposition six weeks post-MI

Masson's trichrome staining was used to evaluate the peri-infarct LV myocardium collagen deposition, which was composed of red normal myocardial cells and blue fibrin component (Figure 3A–3D). At six weeks post-MI, untreated MI rats displayed a large degree of fibrosis compared with control rats (Figure 3E, $p<0.01$). Although RSD alone did not affect collagen deposition in control rats, it was decreased relative to interstitial fibrosis, compared with untreated MI rats (Figure 3E, $p<0.01$).

RSD decreases the expression of Collagen I and Collagen III in LV six weeks post-MI

Immunohistochemical analysis of the peri-infarcted area of LV indicated that untreated MI caused a significant increase in Collagen I and Collagen III compared with the control group (Figure 4A, Figure 5A). The expression of Collagen I and Collagen III was decreased in the MI group treated with RSD (Figure 4A, Figure 5A). Compared with the normal rats, the mRNA and protein expression of both Collagen I and Collagen III was upregulated in the peri-infarct area of LV of MI rats at six weeks, which was decreased after RSD treatment (Figure 4B, 4C, $p<0.01$; Figure 5B, 5C, $p<0.01$).

Downregulation of microRNA21and upregulation of microRNA101a and microRNA133a expressions in LV by RSD six weeks post-MI

As demonstrated in Figure 6, microRNA21 mRNA was upregulated in the border zone of the infarct area post-MI ($p<0.01$), which was attenuated after RSD treatment. The mRNA expression of both microRNA101a and microRNA133a was decreased after MI ($p<0.01$), and this decrease was reversed in RSD-treated MI rats ($p<0.01$ and $p<0.05$, respectively).

Downregulation of CTGF by RSD in the LV six weeks after MI

Six weeks post-MI, immunohistochemistry showed marked CTGF expression in MI rats, compared with rats in the control group. CTGF overexpression was prevented after RSD treatment (Figure 7A). Accordingly, both real-time PCR and Western blot showed that the TGF-β1 expression in the LV was significantly increased after untreated MI, which was inhibited after RSD treatment (Figure 7B, 7C, $p<0.01$).

Indexed in: [Current Contents/Clinical Medicine] [SCI Expanded] [ISI Alerting System] [ISI Journals Master List] [Index Medicus/MEDLINE] [EMBASE/Excerpta Medica] [Chemical Abstracts/CAS] [Index Copernicus]

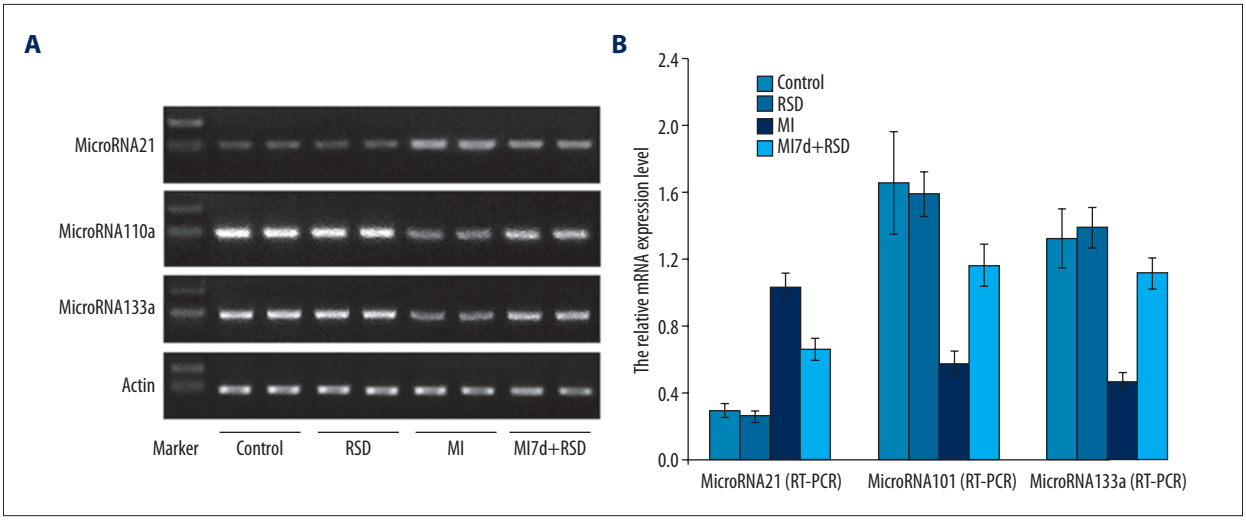

Figure 6. Effect of RSD on microRNA21, microRNA 101a, microRNA 133a in left ventricle (LV) myocardium six weeks post-MI. (**A**) Relative expression of microRNA21, microRNA 101a, and microRNA 133a is detected in LV by real-time RT-PCR; (**B**) The expression of microRNA 101a and microRNA 133a is upregulated, while the expression of microRNA21 is downregulated in the peri-infarct area of LV of RSD-treated rats at six weeks. Data are expressed as mean ± standard deviation. ** $p<0.01$ *vs.* either control or RSD group; # $p<0.05$, ## $p<0.01$ *vs.* MI group, respectively.

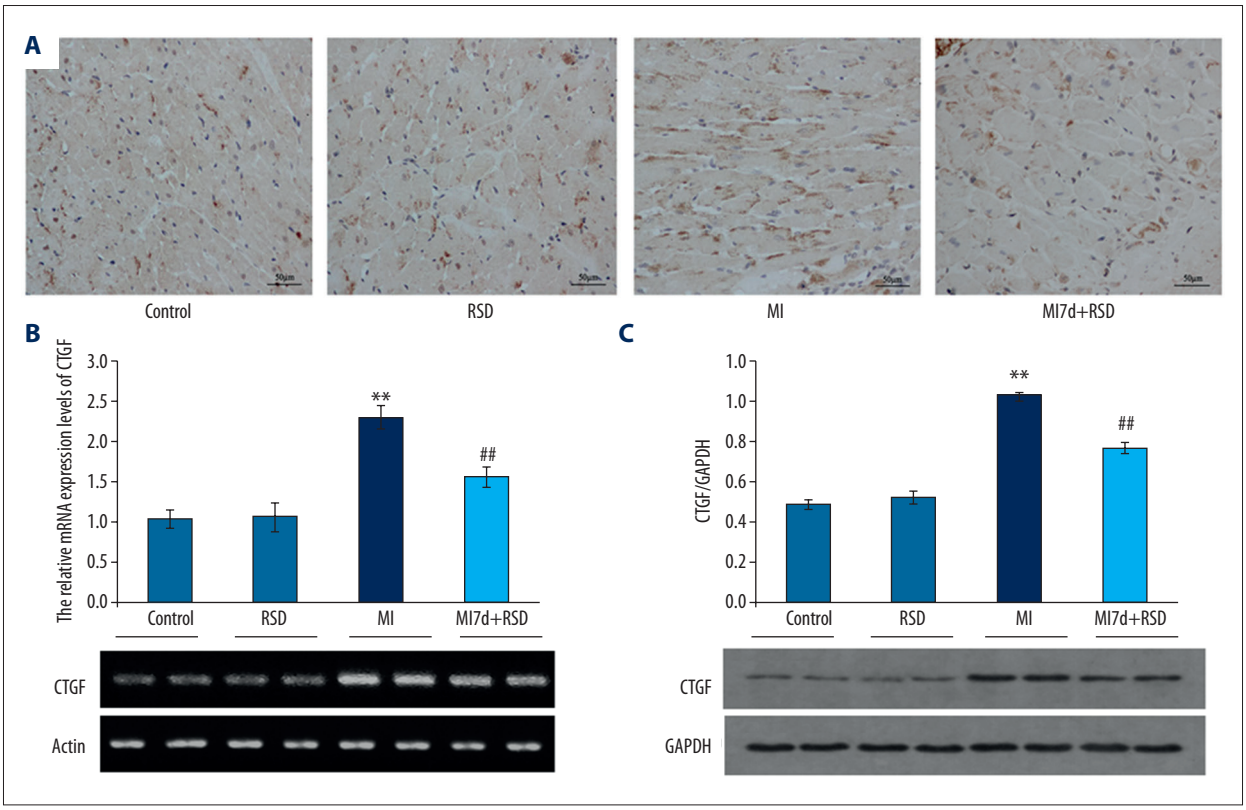

Figure 7. CTGF expression in the remote area of left ventricle six weeks post-MI. (**A**) Immunostaining of CTGF, brown stain, 400×. (**B**) Decreased CTGF mRNA expression is seen in rats treated with RSD compared with that of MI rats by real time RT-PCR. (**C**) Decreased CTGF expression is shown in rats treated with RSD compared with that of MI rats using Western blot. Data are shown as mean ± standard deviation, ** $p<0.01$ *vs.* either control or RSD group, ## $p<0.01$ *vs.* MI group.

Indexed in: [Current Contents/Clinical Medicine] [SCI Expanded] [ISI Alerting System] [ISI Journals Master List] [Index Medicus/MEDLINE] [EMBASE/Excerpta Medica] [Chemical Abstracts/CAS] [Index Copernicus]

Discussion

Neurohumoral factors, especially activated RAAS and SNS, exacerbated ventricular deterioration. Inhibition of RAAS and SNS by RSD may represent an important mechanism in the improvement of cardiac dysfunction after MI [3,4]. In the current study, RSD exerted preventive and therapeutic effects on post-MI cardiac fibrosis, and improved the LV function after MI, including increased EF, decreased LVEDD and LVESD compared with untreated MI rats. RSD treatment also improved LVSP, LVEDP, dP_{min} and dt_{max}, compared with MI rats six weeks post-MI. RSD effectively improved cardiac function and attenuated cardiac remodeling after MI (Figures 1, 2).

Adverse ventricular remodeling post-MI is characterized by excessive deposition of collagen in the myocardium, resulting in myocardial fibrosis. LV function was improved at the cost of increased left ventricular stiffness [5]. In our study, RSD treated MI rats showed decreased collagen deposition (Figure 3) and downregulated the expression of Collagen I and III in the peri-infarct LV (Figures 4, 5), which may improve the diastolic performance of LV. Therefore, the role of RSD in cardiac fibrosis after MI and the potential mechanisms were the focus of this study.

We further investigated the effect of RSD on the expression of microRNA21, microRNA101a, and microRNA133a, which are powerful regulators of pathological events, including cell growth, extracellular matrix remodeling, and cardiac fibrosis [10,17]. In the present study, the higher microRNA21 expression and the lower microRNA101a and microRNA133a expression in cardiac tissue post-MI suggested proteolytic imbalance, which was attenuated after RSD treatment six weeks post-MI, resulting in improvement in cardiac performance.

CTGF, a profibrotic growth factor, is a diagnostic marker and therapeutic target of ECM synthesis and cardiac fibrosis [18]. Reducing CTGF overexpression may be useful in the treatment of heart failure [19]. In this study, high-level expression of CTGF was seen in the MI of rat hearts, while CTGF overexpression was inhibited in RSD-treated rat hearts (Figure 7). In the healthy heart, microRNA101a and microRNA133a are powerful negative regulators of CTGF expression in the heart acting via translational repression and mRNA degradation [9,11,20]. In the current study, both CTGF transcriptional and protein levels in LV were significantly increased in the MI rat model, which were attenuated after RSD treatment. The molecular mechanisms are complex and require further investigation, but several possible interactions exist.

MI is associated with cardiac hypertrophy and fibrosis, which results in reduced cardiac contractility [21]. Overexpression of ECM proteins including collagens, fibrillins, and elastin greatly contributes to the development and progression of cardiac fibrosis [22]. Different microRNAs including microRNA21, microRNA101a, and microRNA133a participate in the regulation of this process. CTGF is one of the most important signaling molecules which are closely related to RAAS and SNS [23]. CTGF overexpression is affected by upregulation of microRNA21 and downregulation of microRNA101a and microRNA133a, leading to myocardial fibrosis [10,11,24–26]. Indeed, the CTGF expression may be affected by RAAS and SNS activation via myocardial microRNA pathways suggesting that a complete feed forward loop developed in cardiac fibrosis and ventricular remodeling. RSD probably regulates microRNAs and subsequent CTGF expression in the inhibition of pathophysiology of ventricular remodeling via its effect on RAAS and SNS in heart tissue.

In our study, in RSD-treated MI rats, the plasma norepinephrine level was increased, along with increased activation of circulating RAAS compared with the MI group (Table 2). The results of the present study are consistent with previous findings with respect to RSD-related reduction in renal norepinephrine spillover and inhibition in RASS activity via blockage of efferent and afferent renal sympathetic nerves [27]. Angiotensin II activates the local RAAS of other organs. It also acts as a positive feedback factor between SNS and RAAS [28]. Therefore, RSD inhibits RAAS and SNS simultaneously to block the neurohormonal activation *in vivo*, which may play a role in anti-HF effects. This mechanism explains our study observations that RSD affected myocardial fibrosis via inhibition of CTGF expression by upregulating microRNA 101a and microRNA 133a and downregulating microRNA21. The current study suggests that RSD may also display therapeutic effects in HF post-MI. However, the precise mechanism underlying improved cardiac function *in vivo* with RSD remains to be established.

Conclusions

This study showed a beneficial effect of RSD on the attenuation of MI-induced increase in SNS and RAAS activities as well as LV fibrosis, which might contribute to LV dysfunction in a rat model after MI. Increased CTGF activity may result in myocardial fibrosis post-MI. The attenuation of collagen depositions after RSD treatment may be due to inhibition of CTGF expression via upregulation of microRNA 101a and microRNA 133a expression and downregulation of microRNA21 expression. Our data indicate that RSD is a promising non-pharmaceutical strategy for MI-induced HF.

Limitations

The changes in local RAAS and SNS activity (such as local angiotensin II receptors and catecholamine levels, beta-adrenergic receptor density and function) were not discussed in the

Indexed in: [Current Contents/Clinical Medicine] [SCI Expanded] [ISI Alerting System] [ISI Journals Master List] [Index Medicus/MEDLINE] [EMBASE/Excerpta Medica] [Chemical Abstracts/CAS] [Index Copernicus]

present study. To some extent, the study was mostly observational and the mechanistic investigations were limited. Further studies are necessary to accurately establish the mechanisms of RSD in the cardiovascular system *in vivo*.

Transforming growth factor-β1 (TGF-β1) is a profibrotic cytokine that accelerates extracellular matrix remodeling after ischemia in LV failure, but it was not investigated in this study. Further conclusions related to TGF-β1 and associated microRNAs will be confirmed in our future studies.

Competing interests

None declared.

References:

1. Roger VL, Go AS, Lloyd-Jones DM et al: Heart disease and stroke statistics – 2012 update: A report from the American Heart Association. Circulation, 2012; 125: e2–e220
2. Paul M, Poyan Mehr A, Kreutz R: Physiology of local renin-angiotensin systems. Physiol Rev, 2006; 86: 747–803
3. Schirmer SH, Sayed MM, Reil JC et al: Atrial remodeling following catheter-based renal denervation occurs in a blood pressure- and heart rate-independent manner. JACC Cardiovasc Interv, 2015; 8: 972–80
4. Thaung HP, Yao Y, Bussey CT et al: Chronic bilateral renal denervation reduces cardiac hypertrophic remodelling but not beta-adrenergic responsiveness in hypertensive type 1 diabetic rats. Exp Physiol, 2015; 100: 628–39
5. French BA, Kramer CM: Mechanisms of post-infarct left ventricular remodeling. Drug Discov Today Dis Mech, 2007; 4: 185–96
6. Guo Z, Zhao Q, Deng H et al: Renal sympathetic denervation attenuates the ventricular substrate and electrophysiological remodeling in dogs with pacing-induced heart failure. Int J Cardiol, 2014; 175: 185–86
7. Hu J, Ji M, Niu C et al: Effects of renal sympathetic denervation on post-myocardial infarction cardiac remodeling in rats. PloS One, 2012; 7: e45986
8. Jiang W, Tan L, Guo Y et al: Effect of renal denervation procedure on left ventricular hypertrophy of hypertensive rats and its mechanisms. Acta Cir Bras, 2012; 27: 815–20
9. Sala V, Bergerone S, Gatti S et al: MicroRNAs in myocardial ischemia: Identifying new targets and tools for treating heart disease. New frontiers for miR-medicine. Cell Mol Life Sci, 2014; 71: 1439–52
10. Thum T, Lorenzen JM: Cardiac fibrosis revisited by microRNA therapeutics. Circulation, 2012; 126: 800–2
11. Duisters RF, Tijsen AJ, Schroen B et al: miR-133 and miR-30 regulate connective tissue growth factor: Implications for a role of microRNAs in myocardial matrix remodeling. Circ Res, 2009; 104: 170–78
12. Chen MM, Lam A, Abraham JA et al: CTGF expression is induced by TGF-beta in cardiac fibroblasts and cardiac myocytes: A potential role in heart fibrosis. J Mol Cell Cardiol, 2000; 32: 1805–19
13. Shi-Wen X, Leask A, Abraham D: Regulation and function of connective tissue growth factor/CCN2 in tissue repair, scarring and fibrosis. Cytokine Growth Factor Rev, 2008; 19: 133–44
14. Spinale FG, Gunasinghe H, Sprunger PD et al: Extracellular degradative pathways in myocardial remodeling and progression to heart failure. J Card Fail, 2002; 8: S332–38
15. Pfeffer MA, Pfeffer JM, Fishbein MC et al: Myocardial infarct size and ventricular function in rats. Circ Res, 1979; 44: 503–12
16. Limana F, Germani A, Zacheo A et al: Exogenous high-mobility group box 1 protein induces myocardial regeneration after infarction via enhanced cardiac C-kit+ cell proliferation and differentiation. Circ Res, 2005; 97: e73–83
17. Castoldi G, Di Gioia CR, Bombardi C et al: MiR-133a regulates collagen 1A1: potential role of miR-133a in myocardial fibrosis in angiotensin II-dependent hypertension. J Cell Physiol, 2012; 227: 850–56
18. Blom IE, Goldschmeding R, Leask A: Gene regulation of connective tissue growth factor: new targets for antifibrotic therapy? Matrix Biol, 2002; 21: 473–82
19. Szabo Z, Magga J, Alakoski T et al: Connective tissue growth factor inhibition attenuates left ventricular remodeling and dysfunction in pressure overload-induced heart failure. Hypertension, 2014; 63: 1235–40
20. Pan Z, Sun X, Shan H et al: MicroRNA-101 inhibited postinfarct cardiac fibrosis and improved left ventricular compliance via the FBJ osteosarcoma oncogene/transforming growth factor-beta1 pathway. Circulation, 2012; 126: 840–50
21. van Rooij E, Sutherland LB, Thatcher JE et al: Dysregulation of microRNAs after myocardial infarction reveals a role of miR-29 in cardiac fibrosis. Proc Natl Acad Sci USA, 2008; 105: 13027–32
22. Watson CJ, Horgan S, Neary R et al: Epigenetic therapy for the treatment of hypertension-induced cardiac hypertrophy and fibrosis. J Cardiovasc Pharmacol Ther, 2016; 21(1): 127–37
23. Linz D, Hohl M, Nickel A et al: Effect of renal denervation on neurohumoral activation triggering atrial fibrillation in obstructive sleep apnea. Hypertension, 2013; 62: 767–74
24. Accornero F, van Berlo JH, Correll RN et al: Genetic analysis of connective tissue growth factor as an effector of transforming growth factor beta signaling and cardiac remodeling. Mol Cell Biol, 2015; 35: 2154–64
25. Sayed D, Rane S, Lypowy J et al: MicroRNA-21 targets Sprouty2 and promotes cellular outgrowths. Mol Biol Cell, 2008; 19: 3272–82
26. Dai Y, Khaidakov M, Wang X et al: MicroRNAs involved in the regulation of postischemic cardiac fibrosis. Hypertension, 2013; 61: 751–56
27. Jorde UP: Suppression of the renin-angiotensin-aldosterone system in chronic heart failure: Choice of agents and clinical impact. Cardiol Rev, 2006; 14: 81–87
28. Jabaudon D, Shnider SJ, Tischfield DJ et al: RORβ induces barrel-like neuronal clusters in the developing neocortex. Cereb Cortex, 2012; 22(5): 996–1006

Indexed in: [Current Contents/Clinical Medicine] [SCI Expanded] [ISI Alerting System] [ISI Journals Master List] [Index Medicus/MEDLINE] [EMBASE/Excerpta Medica] [Chemical Abstracts/CAS] [Index Copernicus]